# EFFECT OF FASTENING ON THE MICROSTRUCTURE OF CARBON FIBER POLYMER-MATRIX COMPOSITES

Chia-Ken Leong, Shoukai Wang and D.D.L. Chung
*Composite Materials Research Laboratory*
*University at Buffalo*
*State University of New York*
*Buffalo, NY 14260-4400, U.S.A.*

## Introduction

Continuous carbon fiber epoxy-matrix composites are important for lightweight structures. Fastening is a common method of joining composite components. In the case of composite laminates, fastening involves compression in the direction perpendicular to the laminae. The effect of fastening on the microstructure of composite laminates is of current aircraft safety concern, due to the 2001 Airbus accident in New York. The accident involved degradation of the fastening between the tail and the body of the aircraft.

Considerable prior attention has been given to studying the effect of tension in the fiber direction of a composite on the microstructure of the composite [1-6]. This is because the fiber direction is the strong direction of the composite and the composite is stronger under tension than compression in this direction. In contrast, this paper is focused on the effect of compression in the through-thickness direction, due to its relevance to fastening.

Due to the electrical conductivity of carbon fiber, electrical resistance measurement is effective for monitoring the microstructural changes in a carbon fiber composite [1-9]. This method is also advantageous in its nondestructive nature, fast response, equipment simplicity and applicability to large structural components.

This paper uses DC electrical resistance to monitor the effect of repeated compression in the through-thickness direction at various stress amplitudes (equivalent to repeated fastening and unfastening at various loads) on the microstructure of the interlaminar interface (i.e., the interface between adjacent laminae) and on that within a lamina. The effect on the microstructure of the interlaminar interface was studied by measuring the contact electrical resistivity of the interface [10-12]. The effect on the microstructure of a lamina was studied by measuring the volume resistance of a lamina in both the longitudinal and transverse directions.

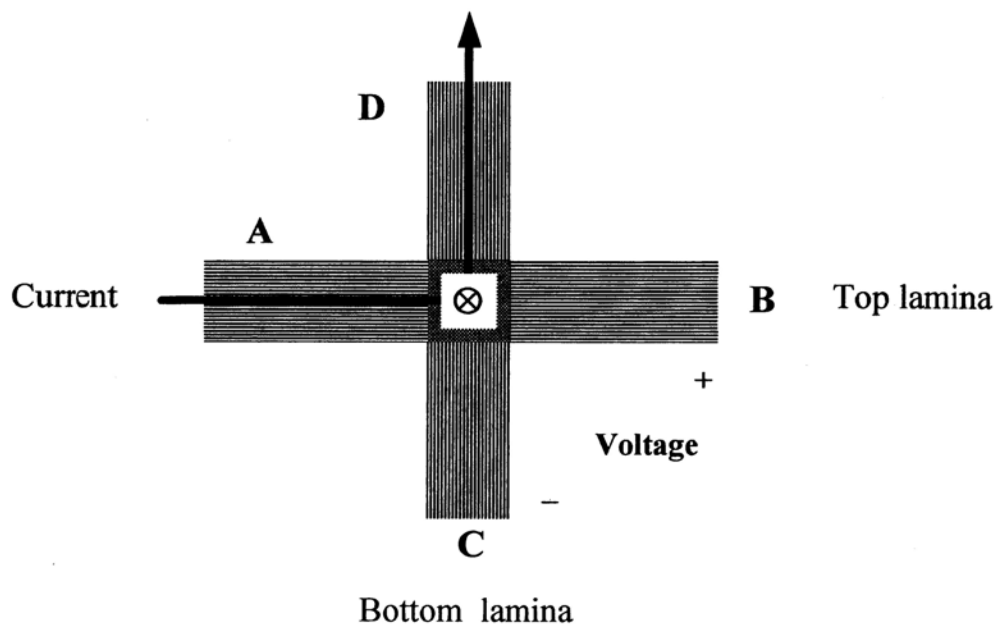


Fig. 1 Composite configuration for measuring the contact electrical resistivity of the interlaminar interface. A and D are current contacts; B and C are voltage contacts.

## Experimental methods

The composites were made from unidirectional carbon fiber epoxy-matrix prepregs.

For measuring the contact resistivity of the interlaminar interface, two laminae of prepreg in the form of strips crossing one another, with one strip on top of the other (Fig. 1), were fabricated into a composite at the overlapping region (ranging from 3 x 3 to 6 x 6 mm) of the two laminae by applying pressure and heat to the overlapping region (without a mold).

For measuring the volume resistance of a lamina in both longitudinal and transverse directions, a single lamina of prepreg was cut into the shape of a cross, as shown in Fig. 2. After the cutting, the composite was cured by hot pressing.

In both Fig. 1 and 2, the resistance was measured by using the four-probe method. In this method, the outer two contacts are for passing the current, while the inner two contacts are for measuring the voltage.

A dynamic compressive stress was applied on the square region in the middle of Fig. 1 and 2 by using a hydraulic mechanical testing system (MTS 810, MTS Systems Corp., Marblehead, MA). Simultaneously, the resistance was

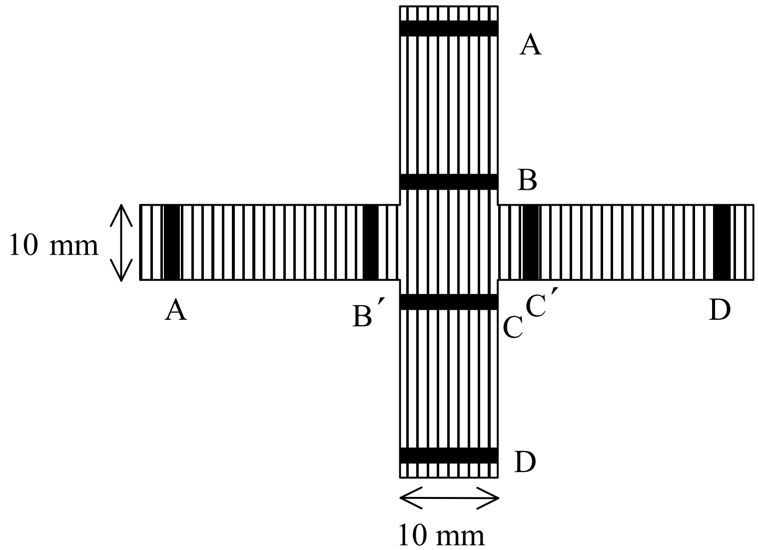


Fig. 2 Composite configuration for measuring the volume electrical resistance of a single lamina in both the longitudinal and transverse directions. A and D are current contacts, while B and C are voltage contacts, all for measuring the longitudinal volume resistance. A′ and D′ are current contacts, while B′ and C′ are voltage contacts, all for measuring the transverse volume resistance. All dimensions are in mm. The distance between A and D and that between A′ and D′ are 80 mm. The distance between B and C and that between B′ and C′ are 20 mm.

measured. In the case of Fig. 2, the longitudinal and transverse resistances were measured simultaneously.

Because the compressive strain in Fig. 2 was not measured, the volume resistivity was not determined. Nevertheless, the measured volume resistance gives valuable information.

**Results and discussion**

<u>Effect on the microstructure of the interlaminar interface</u>

Fig. 3 shows the variation of the contact resistivity with stress during compressive stress cycling to various maximum stresses up to 4 MPa. The composite was made at a curing pressure of 0.43 MPa. The contact resistivity decreased quite reversibly upon loading, due to the increased contact between fibers of adjacent laminae. However, the resistivity decrease was not completely reversible. The greater the stress, the more the contact resistivity decreased. Although Fig. 3

shows results at stress amplitudes up to 4 MPa, similar results were obtained up to 26 MPa.

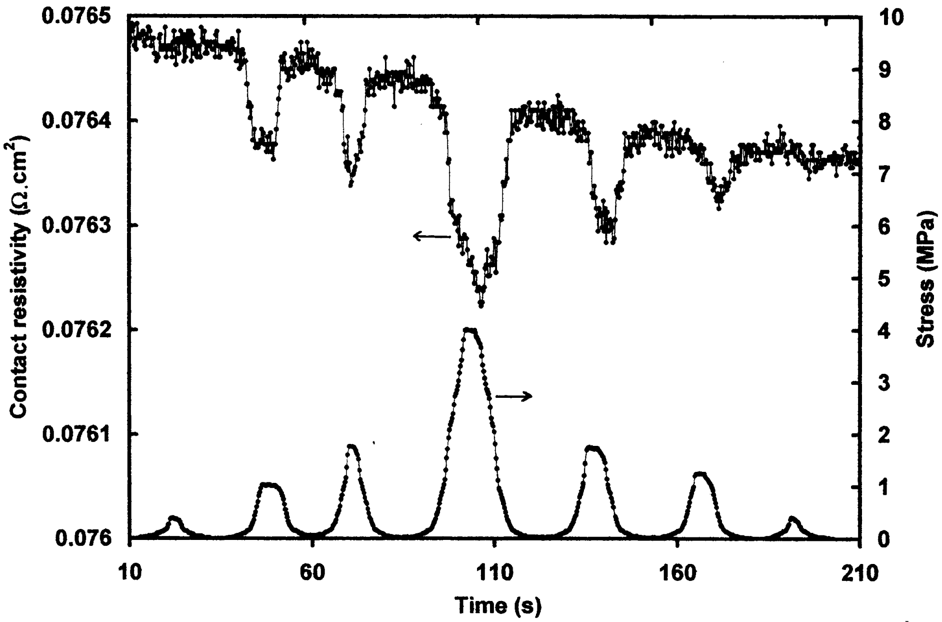


Fig. 3 Variation of the contact electrical resistivity with time and of the stress with time during stress cycling to different stress amplitudes up to 4 MPa. The specimen configuration is that in Fig. 1.

Effect on the microstructure of a laminae

Fig. 4 shows the variation of the longitudinal resistance during dynamic compression at progressively increasing stress amplitudes up to fracture, such that three stress cycles were conducted at each stress amplitude. The resistance decreased upon compressive loading, in spite of the expected accompanying decrease in thickness (not measured) tending to cause the resistance to increase. The resistance decrease is attributed to the fiber squeezing (i.e., increase in the extent of fiber-fiber contact) in the through-thickness direction and the consequent decrease in the through-thickness volume resistivity (not measured). A decrease in the through-thickness resistivity is expected to cause the longitudinal resistivity to decrease, due to the increased chance of the current to detour from one fiber to an adjacent fiber. This detour would enhance the longitudinal conductivity in case that some fibers are damaged. The effect is reversible, as shown upon unloading.

As the stress amplitude increased, the amplitude of resistance change increased, as expected. Among the three cycles at the same stress amplitude, the amplitude of resistance change was higher in the first cycle than the subsequent two cycles. At any particular stress amplitude, the resistance decrease during loading in the first cycle was followed upon subsequent unloading by a resistance increase such that the resistance after unloading was substantially higher than

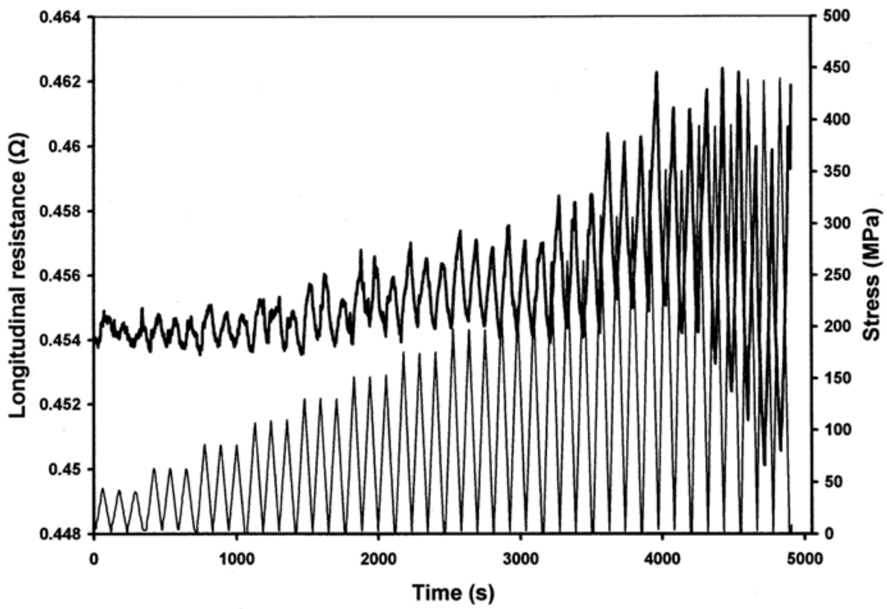


Fig. 4 Variation of the longitudinal volume electrical resistance with time (thick curve) and of the stress with time (thin curve) during stress cycling at progressively increasing stress amplitudes up to 450 MPa. Fracture was observed at the end of this test.

that before the first loading at this stress amplitude. This indicates damage (or an irreversible microstructural change) occurring during unloading in the first cycle at this stress amplitude. In the subsequent two cycles at this stress amplitude, no further damage was inflicted, as indicated by the absence of additional resistance increase during unloading in each of these cycles. The damage (or irreversible microstructural change) was of a type that caused the longitudinal resistance to increase. It may relate to fiber damage, since fiber damage is expected to increase the longitudinal resistance. As expected, a greater extent of microstructural change (or damage) occurred when a stress amplitude was experienced for the first time.

Fig. 5 shows the corresponding results on the transverse volume resistance. At stress amplitudes up to 310 MPa, the resistance increased upon loading in every cycle. This is due to fiber spreading, i.e., increase of the average distance between adjacent fibers in the transverse direction. This effect is largely reversible. It is less reversible for the first cycle than the subsequent two cycles at the same stress amplitude. Moreover, the amplitude of resistance change was larger for the first cycle than the subsequent two cycles, due to more fiber spreading when a stress amplitude was experienced for the first time.

During unloading, the resistance decreased. Upon subsequent loading, the resistance continued to decrease, as shown in Fig. 6, which is a magnified view of a part of Fig. 5. This continued decrease in resistance is due to the increased

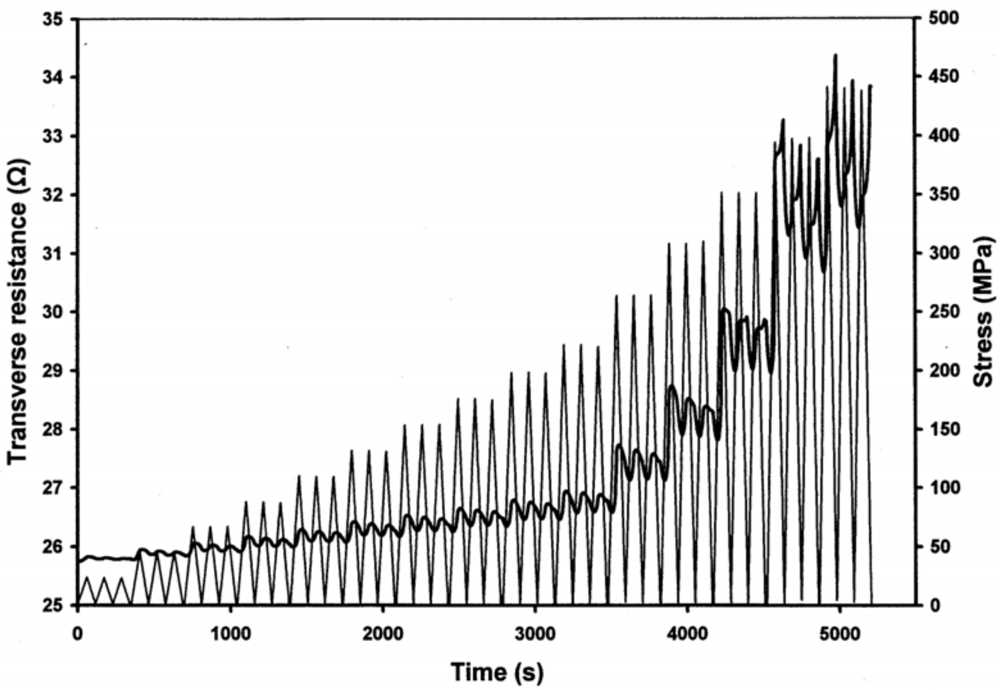


Fig. 5 Variation of the transverse volume electrical resistance with time (thick curve) and of the stress with time (thin curve) during stress cycling at progressively increasing stress amplitudes up to 450 MPa. Fracture was observed at the end of this test.

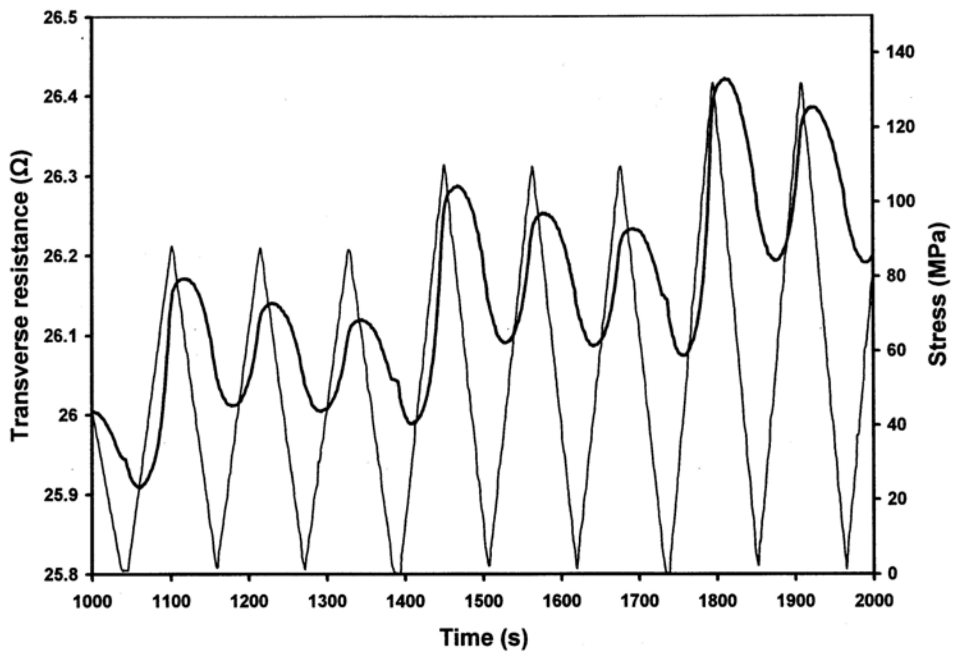


Fig. 6 Magnified view of a part of Fig. 5.

extent of fiber-fiber contact in the through-thickness direction. After the reloading had reached an intermediate level, the resistance started to increase, due to fiber spreading. In other words, there were two microstructural effects, i.e., fiber spreading in the transverse direction and fiber squeezing in the through-thickness direction. Fiber spreading was the dominant phenomenon, but both phenomena occurred in each stress cycle.

At stress amplitudes above 310 MPa, the resistance started to increase when unloading was near completion, thereby resulting in a spike at zero load. This effect is due to the lessening of fiber squeezing in the through-thickness direction. At stress amplitudes above 350 MPa, this spike was the dominant effect in a cycle, i.e., the phenomenon associated with the lessening of fiber squeezing in the through-thickness direction overshadowed the phenomenon associated with fiber spreading in the transverse direction, probably because the fiber spreading had reached its limit. In other words, fiber spreading was the dominant effect at stress amplitudes up to 350 MPa, but the lessening of fiber squeezing in the through-thickness direction was the dominant effect at stress amplitudes above 350 MPa.

Fig. 5 also shows that the baseline transverse resistance increased as the stress amplitude increased. The increase was gradual at stress amplitudes up to 230 MPa, but was increasingly abrupt as the stress amplitude increased beyond 230 MPa. This baseline increase is probably due to damage in the form of matrix cracks between adjacent fibers.

It should be noted that the stress amplitudes in this section are much higher than those in the last section. This means that the microstructure of the interlaminar interface required much less stress in order for it to be changed than the microstructure within a lamina, as expected.

## Conclusion

Compression in the through-thickness direction (as in fastening) of a carbon fiber epoxy-matrix composite caused the extent of fiber-fiber contact across the interlaminar interface to increase, as shown by decrease in the contact resistivity of this interface. The effect was not totally reversible, even at a small stress amplitude of 1 MPa.

For a single lamina, this compression caused fiber squeezing in the through-thickness direction, as shown by decrease in the longitudinal volume resistance. Accompanying this effect was fiber spreading in the transverse direction, as shown by increase in the transverse volume resistance. Both effects were reversible, though slight and partial irreversibility was observed at the first experience of a stress amplitude of 100 MPa or above.

For a single lamina, as the stress amplitude increased to 400 MPa, the lessening of fiber squeezing in the through-thickness direction during unloading started to dominate over the fiber spreading in the transverse direction during loading, as shown by the transverse volume resistance increasing upon unloading starting to dominate over the competing phenomenon in which this resistance increased upon loading. This is because of the fiber spreading approaching its limit as the stress amplitude increased.

## References

[1] Wang X, Chung DDL. Continuous carbon fiber epoxy-matrix composite as a sensor of its own strain. Smart Mater Struct 1996;5:796-800.
[2] Wang X, Chung DDL. Real-time monitoring of fatigue damage and dynamic strain in carbon fiber polymer-matrix composite by electrical resistance measurement. Smart Mater Struct 1997;6:504-508.
[3] Wang X, Chung DDL. Self-monitoring of fatigue damage and dynamic strain in carbon fiber polymer-matrix composite. Composites: Part B 1998;29B(1):63-73.
[4] Wang X, Fu X, Chung DDL. Electromechanical study of carbon fiber composites. J Mater Res 1998;13(11):3081-3092.
[5] Wang X, Chung DDL. Fiber breakage in polymer-matrix composite during static and dynamic loading, studied by electrical resistance measurement. J Mater Res 1999;14(11):4224-4229.
[6] Wang S, Chung DDL. Piezoresistivity in continuous carbon fiber polymer-matrix composites. Polymer Composites 2000;21(1):13-19.

[7] Wang X, Wang S, Chung DDL. Sensing damage in carbon fiber and its polymer-matrix and carbon-matrix composites by electrical resistance measurement. J Mater Sci 1999;34(11):2703-2714.
[8] Wang S, Chung DDL. Electrical behavior of carbon fiber polymer-matrix composites in the through-thickness direction. J Mater Sci 2000;35(1):91-100.
[9] Wang X, Chung DDL. An electromechanical study of the transverse behavior of carbon fiber polymer-matrix composite. Composite Interfaces 1998;5(3):191-199.
[10] Wang S, Chung DDL. Interlaminar interface in carbon fiber polymer-matrix composites, studied by contact electrical resistivity measurement. Composite Interfaces 1999;6(6):497-506.
[11] Wang S, Chung DDL. Interlaminar shear in carbon fiber polymer-matrix composites, studied by measuring the contact electrical resistance of the interlaminar interface during shear. Composite Interfaces 1999;6(6):507-518.
[12] Wang S, Chung DDL. Thermal fatigue in carbon fiber polymer-matrix composite, monitored in real time by electrical resistance measurement. Polymers & Polymer Composites 2001;9(2):135-140.